Title

A cellular basis for heightened gut sensitivity in females

Journal

Science, 390(6779)

ISSN

0036-8075

Authors

Venkataraman, Archana
Figueroa, Eric E
Castro, Joel
et al.

Publication Date

2025-12-18

DOI

10.1126/science.adz1398

HHS Public Access

Author manuscript

Science. Author manuscript; available in PMC 2026 March 17.

Published in final edited form as:

Science. 2025 December 18; 390(6779): 1285–1291. doi:10.1126/science.adz1398.

A Cellular Basis for Heightened Gut Sensitivity in Females

Archana Venkataraman[1,†], **Eric E. Figueroa**[2,†], **Joel Castro**[3,4], **Fernanda M. Castro Navarro**[1], **Deepanshu Soota**[1], **Stuart M. Brierley**[3,4], **David Julius**[2,*], **Holly A. Ingraham**[1,*]

[1] Department of Cellular and Molecular Pharmacology, University of California, San Francisco, CA 94143, USA

[2] Department of Physiology, University of California, San Francisco, CA 94143, USA

[3] Hopwood Centre for Neurobiology, Lifelong Health, South Australian Health and Medical Research Institute (SAHMRI); North Terrace, Adelaide, SA 5000, AUSTRALIA

[4] Faculty of Health and Medical Sciences, University of Adelaide; North Terrace, Adelaide, South Australia 5000, AUSTRALIA

Abstract

Visceral pain disorders, such as irritable bowel syndrome, exhibit a marked female prevalence. Enhanced signaling between enterochromaffin (EC) cells in the gut epithelium and mucosal sensory nerve fibers likely contributes to this sex bias. We identified an estrogen-responsive paracrine pathway in which two enteroendocrine cell types, peptide YY (PYY)-expressing L cells and serotonergic EC cells, communicate to increase gut sensitivity in females. We demonstrate that estrogen signaling up-regulates the bacterial metabolite short-chain fatty acid receptor *Olfr78* on colonic L cells, increasing PYY release and their sensitivity to acetate. Elevated PYY acts on neighboring EC cells by means of NPY1R, thereby enhancing serotonin release and gut pain. We propose that hormonal fluctuations, in conjunction with internal (stress) or environmental (diet) factors, amplify this local estrogen-responsive colonic circuit, resulting in maladaptive gut sensitivity.

Chronic gastrointestinal pain conditions, such as irritable bowel syndrome (IBS), are more prevalent in women (1, 2) and can be exacerbated by fluctuating estrogen levels during the menstrual cycle and pregnancy (3, 4). Although relevant targets of estrogen have not been identified, one possible site of action is the gut mucosa, in which sensory nerve fibers communicate with epithelial cells to detect noxious stimuli and transmit nociceptive information to the spinal cord. Most epithelial cells that line the gut are enterocytes that primarily function to absorb nutrients, water, and electrolytes from the digestive tract. Interspersed among these enterocytes are rare, excitable enteroendocrine cells (EECs) that

[*]**Corresponding author.** holly.ingraham@ucsf.edu (H.A.I.); david.julius@ucsf.edu (D.J.).
[†]These authors contributed equally to this work.

Author contributions: Conceptualization: A.V., E.E.F., D.J., S.M.B., and H.A.I. Methodology: A.V., E.E.F., J.C., F.M.C.N., and D.S. Investigation: A.V., E.E.F., J.C., and F.M.C.N. Visualization: A.V., E.E.F., J.C., F.M.C.N., D.S., H.A.I., and S.M.B. Funding acquisition: E.E.F., H.A.I., D.J., S.M.B., and J.C. Supervision: H.A.I., D.J., and S.M.B. Writing – original draft: A.V., E.E.F., D.J., and H.A.I. Writing – review and editing: A.V., E.E.F., D.J., H.A.I., J.C., and S.M.B.

Competing interests:
The authors declare that they have no competing interests.

detect luminal contents (including nutrients, microbial metabolites, and ingested irritants) and release peptides and neurotransmitters to elicit an array of physiological responses. Serotonergic enterochromaffin (EC) cells are a distinct subtype of EECs that activate neighboring mucosal spinal afferents to elicit visceral pain (5–7). This EC cell-sensory nerve circuit shows heightened sensitivity in female mice (5), raising the possibility that it is a locus for hormone-dependent enhancement of visceral pain. Whether and how estrogen acts to modulate this peripheral pain circuit remains unclear.

The L cell, another well-characterized EEC subtype, is primarily recognized for its role in sensing postprandial nutrients and secreting hormones such as glucagon-like peptide-1 (GLP-1) and peptide YY (PYY) to regulate insulin secretion, digestion, gastrointestinal motility, and absorption (8). Although the sites of GLP-1 action are numerous, it is postulated to act locally through activation of GLP-1 receptors on EC cells to trigger the release of serotonin (9). However, unlike GLP-1, a role for PYY (specifically the cleaved $PYY_{3–36}$ peptide) in promoting negative energy balance and appetite suppression (10, 11) is less clear (12, 13). When given exogenously, $PYY_{3–36}$ results in marked gastrointestinal (GI) discomfort in humans (14, 15) and food aversion in rodents (16). Whereas $PYY_{3–36}$ selectively binds to NPY2 receptors in vagal afferents (17) and the brain (18), the larger $PYY_{1–36}$ peptide additionally activates the NPY1 receptors (19), which in the gut are expressed by EC cells and spinal afferents (9). With EC cells emerging as the main detectors of noxious stimuli in the gut epithelium, coupling between $PYY_{1–36}$ and NPY1R would presumably lead to visceral discomfort and hypersensitivity by increasing serotonin release, as originally hypothesized by Kojima and colleagues (20). However, given the intense focus on L cells (and PYY) as nutrient sensors in the small intestine, few if any studies have explored paracrine coupling between L and EC cells in the colon and consequent effects on visceral pain. We show that cellular crosstalk between L and EC cells leads to visceral hypersensitivity, revealing a role for $PYY_{1–36}$ as a major nociceptive transmitter in the colon. This inter-enteroendocrine conduit is co-opted by estrogen by means of estrogen receptor alpha (ERα) on L cells, revealing a mechanism to account for visceral hypersensitivity in females.

Results

ERα is required for heightened visceral sensitivity in females

We have previously shown that mucosal sensory afferents exhibit higher baseline activity in female mice compared with male mice (5). To determine whether estrogen plays a role in this differential sensitivity, we compared afferent nerve fiber activity in ex vivo mucosal preparations (evMAR) from males versus intact or ovariectomized (OVX) females. Indeed, mechanical stimulation of the mucosa elicited higher responses in females compared with males, and this difference was greatly attenuated by OVX (Fig. 1, A and B, and fig. S1, A and B). Similar results were obtained with evMAR preparations from mice (*$Na_V1.8$-ChR2*) expressing channelrhodopsin in sensory afferents, where spiking was observed at substantially lower light intensities for intact females compared with OVX females (Fig. 1C and fig. S1C).

Estrogen also had a marked effect on behavioral measures of visceral sensitivity as determined by assessing visceral motor responses (VMRs) to colorectal distension (21, 22), akin to how pain is evaluated in patients with IBS (23). Responses in females were significantly blunted when estrogen was depleted by OVX ($P < 0.0001$) (Fig. 1D). A single treatment of OVX females with estradiol benzoate (EB) reversed this drop, with maximum effects observed at 6 hours following EB injection ($P = 0.0018$) (Fig. 1E and fig. S1D). Similarly, the low baseline VMR responses in males were also enhanced by this hormone treatment (Fig. 1F and fig. S1E). Together, these results establish that estrogen, whether endogenous or exogenous, maintains a heightened state of gut sensitivity in females. In this regard, we observed that the dominant transducer of estrogen, namely estrogen receptor alpha (ERα, encoded by the *Esr1* gene) was expressed at relatively low levels in proximal gut regions, but at much higher levels in a sparse population of cells within the colonic epithelium, particularly in the distal colon of females and males where visceral pain is most acutely sensed (Fig. 1, G and H). To assess how loss of ERα affects gut function and visceral sensitivity, we crossed a *Vil1-Cre* driver to the floxed $Esr1^{fl/fl}$ allele to eliminate ERα in the entire intestinal epithelium (Fig. 2A and fig. S2A). Gross metabolic parameters, including body weight and daily food intake, remained unchanged in mutant mice (Fig. 2B and fig. S2, B and C). However, colonic motility and GI transit times ($P < 0.0001$) were substantially accelerated, especially in females (Fig. 2, C and D), as predicted from known effects of estrogen on gut motility (24). Further, depleting intestinal ERα markedly lowered mucosal afferent sensitivity in females compared with males (Fig. 2E and fig. S2D). This lowered sensitivity was mirrored in VMR assays as $Esr1^{Vil1\text{-}Cre}$ females were largely unresponsive until higher distension pressures (60 to 80 mmHg) compared to $Esr1^{fl/fl}$ controls (Fig. 2F); circulating serotonin levels were also lower in mutant females (Fig. 2G). Especially notable was the inability of estrogen treatment to increase visceral sensitivity in $Esr1^{Vil1\text{-}Cre}$ females, compared with their littermate controls (Figs. 1E and 2H). These data establish that ERα is essential for the estrogen-dependent enhancement of visceral sensitivity.

Given their role in driving visceral sensitivity, we presumed ERα would reside in EC cells, but we instead found the receptor absent (fig. S3A). Although unexpected, this finding is consistent with the fact that very few estrogen-responsive genes were detected in EC cells (fig. S3B) and the number of EC cells was unchanged across the estrous cycle (fig. S3C). Instead, we found that *Esr1* expression overlaps with 100% of *Pyy*- (and *Cck*-) expressing cells, especially in the distal colon; overlap with *Gcg,* which encodes GLP-1, was limited (Fig. 2, I and J, and fig. S3, D to F).

PYY-induced visceral pain increased with estrogen

Given the restricted expression of *Esr1* in L cells, we asked whether estrogen promotes visceral pain by increasing L cell secretion of PYY and/or GLP-1, both of which have been proposed to enhance serotonin release by activation of their cognate G protein-coupled receptors on EC cells (9, 20). In intact female mice, we found a marked increase in circulating PYY peaking 6 hours following estrogen treatment (Fig. 3A), whereas GLP-1 and CCK concentrations were largely unaffected (Fig. 3B and fig. S3G) in this setting, even though estrogen has been shown to increase GLP-1 secretion (25). Total PYY levels

remained unchanged at baseline for males and females (fig. S3H) and upon EB treatment in knockout (KO) females (fig. S3I). After first confirming expression of *Npy1r* on nociceptive EC cells (Fig. 3C), as reported by others (9, 26), we asked whether $PYY_{1–36}$ might act downstream of estrogen signaling in L cells to enhance visceral sensitivity in female mice. Indeed, following the addition of $PYY_{1–36}$ to the *Na_V1.8-ChR2* evMAR nerve-gut preparation, a prominent leftward shift was observed after light stimulation in OVX females (Fig. 3D and fig. S4, A and B). Moreover, $PYY_{1–36}$ elicited increased afferent sensitivity to mechanical stimulation in OVX females (Fig. 3E and fig. S4, C and D). Of note, PYY failed to increase the higher baseline sensitivity in intact females (Fig. 3, F and G), but did increase visceral sensitivity in $Esr1^{Vil1\text{-}Cre}$ KO mutant females and control males (fig. S5, A and B). VMR responses to $PYY_{1–36}$ were also significantly elevated in OVX control females ($P = 0.0005$) and ERα KO mutant females ($P = 0.0006$) (Fig. 3, H and I). These findings establish that $PYY_{1–36}$ fully restores gut sensitivity following estrogen depletion in OVX females or after loss of estrogen signaling in the gut epithelium. $PYY_{1–36}$ also increased afferent sensitivity in intact males, whereas GLP-1 failed to show any such effects in males or females (Fig. 3, J and K, and fig. S5C). Collectively, these data support the notion that the estrogen-induced PYY release from L cells directly affects the EC-mucosal afferent circuit to increase visceral sensitivity.

A local paracrine circuit mediates visceral pain in females

To determine whether PYY directly activates EC cells, we used live imaging of intestinal organoids engineered to express an EC cell specific calcium reporter ($Polr2a\text{-}GCaMP5g^{Tac1Cre}$). Robust $PYY_{1–36}$-evoked signals were detected in male $Polr2a\text{-}GCaMP5g^{Tac1Cre}$ organoids (Fig. 4A), and these were blocked by the NPY1R-specific antagonist, BIBO3304 (Fig. 4B and fig. S6A). Similar responses were also detected in female organoids (Fig. 4, C and D and fig. S6B). By contrast, $PYY_{3–36}$ failed to elicit equivalent responses, again consistent with activation of the NPY1R subtype (Fig. 4E). Using a sniffer cell assay (6, 27) in which HEK293T cells express the $gGRAB_{5\text{-}HT3.0}$ serotonin sensor (28), we found that $PYY_{1–36}$ promotes robust serotonin release from EC cells. When sniffer cells were co-cultured with $Polr2a\text{-}GCaMP5g^{Tac1Cre}$ organoids, $PYY_{1–36}$-evoked serotonin release and calcium responses in EC cells were seen to be time-locked (Fig. 4, F and G, and movie S1). Together, these cellular assays demonstrate that L cell derived $PYY_{1–36}$ activates EC cells to elicit serotonin release, confirming previous studies measuring bulk transmitter levels (20). Blocking the NPY1R receptors in our ex vivo and in vivo assays yielded similar results. Indeed, following BIBO3304 treatment, mucosal afferent responses in gut-nerve recordings from intact females were significantly reduced ($P < 0.0001$) (Fig. 4H and fig. S6C), an effect that was not observed in males (fig. S6, D and E). Moreover, estrogen-induced visceral sensitivity in OVX female mice was attenuated to baseline levels following BIBO3304 treatment (Fig. 4I).

To establish that $PYY_{1–36}$ enhances mucosal afferent activity by means of serotonergic signaling, we administered $PYY_{1–36}$ in combination with alosetron, a $5\text{-}HT_3R$ antagonist that is used clinically in women to mitigate IBS symptoms (29). Alosetron abrogated the $PYY_{1–36}$-evoked sensitization of mechanical responses in gut-nerve recordings from OVX females (Fig. 5A and fig. S7, A and B). These findings were recapitulated in vivo,

where alosetron, given 20 min before testing, effectively blocked estrogen-induced visceral sensitivity in OVX females (Fig. 5B). Taken together, these data demonstrate that L cell derived $PYY_{1–36}$ acts locally to promote serotonin release and elicit gut pain by enhancing activity of the EC-mucosal afferent circuit.

Estrogen sensitizes L cell response to SCFAs via OLFR78

Next, we identified estrogen-responsive targets that might modulate visceral sensitivity by profiling sorted tdTomato-expressing L cells (*CckCre-tdTomato*) obtained from EB- or vehicle-treated OVX females. In contrast to the minor effects of estrogen on EC cell gene expression (fig. S3B and table S1), multiple estrogen-sensitive targets were identified in L-cells, including known ERα targets (*Ccnd2, Cdc20,* and *Muc1*), with many more up-regulated (238) than down-regulated (35) (Fig. 5C, and fig. S8A, and tables S2 to S4). Although *Cck* was up-regulated, it failed to engage the L-EC cell pathway (fig. S8, B and C) as was shown for PYY. The short-chain fatty acid (SCFA) receptor encoded by *Olfr78* emerged as another top hit, and its appearance in colonic L-cells after estrogen treatment was confirmed, as was the expression of Epithelial Sodium Channel (ENaC) subunit, *Scnn1g* (Fig. 5, C to E, and fig. S8, D and E). By contrast, *Olfr78* was unchanged in sorted EC cells following estrogen treatment (table S1). To assess whether up-regulation of *Olfr78* is functionally relevant, female colonoids from *Polr2a-GCaMP5g*^{PyyCre} were preincubated with estradiol (E2) for 6 hours and then treated with acetate, the highest-affinity ligand for OLFR78 (30–32). Preincubating colonoids with estrogen significantly elevated L-cell responses to acetate ($P = 0.0019$) (Fig. 5F). Collectively, our data suggest that the hormonal induction of *Olfr78* contributes to sensitization of the female gut through enhanced detection of bacterial metabolites.

Discussion

In this study, we have shown how estrogen signaling modulates paracrine interaction between two enteroendocrine cell types, elucidating a mechanism to explain heightened visceral sensitivity in females (Fig. 5G). $PYY_{1–36}$ released from colonic L cells initiates this cellular cascade by enhancing serotonergic tone in EC cells, leading to activation of nearby 5-HT_3R-expressing mucosal spinal afferents. Estrogen plays a crucial role in triggering these cellular events by i) increasing PYY release from L cells and ii) enhancing the sensitivity of L cells to bacterial metabolites through the up-regulation of the SCFA receptor, *Olfr78,* whose segmental distribution resembles that of *Esr1* in the intestine (33). Our findings also position EC cells as vital coincidence detectors in the gut-brain axis, corroborating earlier studies that paracrine interactions between L and EC cells increase serotonergic signaling, thereby affecting food intake (9), gut motility (34), and now visceral pain, as previously hypothesized (20).

Based on our pharmacological observations –namely, that estrogen enhances PYY release and that blocking NPY1R eliminates heightened visceral sensitivity in intact females or after restoring estrogen in OVX females– we place estrogen directly upstream of $PYY_{1–36}$-NPY1R signaling in EC cells. A local paracrine L-EC-sensory afferent signaling pathway, rather than direct action of PYY on NPY1Rs on spinal afferents (35), is further supported

by the fact that the sensitizing effects of estrogen or PYY on visceral tone are abolished by antagonism of 5-HT_3R. Based on our ability to further sensitize visceral responses by PYY administration in males but not females, we posit that although the estrogen-responsive L-EC sensory pathway is present in both sexes, high estrogen continuously engages this circuit in females, consistent with the higher rates of self-reported IBS in premenopausal women (1, 36). Although total circulating PYY levels showed no significant sex differences, the more relevant measure will be to assess the spatial and temporal dynamics of $PYY_{1–36}$ release within the colon, which will require the development of selective sensors. Our results, together with previous studies (32), may now explain why diets low in fermentable carbohydrates (broadly known as FODMAPs) are beneficial to some individuals who suffer from functional gut disorders (37). Furthermore, our results identify potential new therapeutic targets for such disorders, while also clarifying conflicting views on the role of PYY in appetite suppression when viewed in the context of the colon and gut pain. We suggest that within the colon, PYY is less important as a postprandial signal and instead functions as a nociceptive gut hormone that modulates pain and discomfort, as previously suggested (38). The enrichment of ERα/PYY/*Olfr78*-positive cells in the colon versus the small intestine (32, 33, 39) supports the notion that this estrogen-responsive molecular circuit is functionally positioned to sense and respond to environmental or endogenous noxious stimuli, especially in females.

Our study predicts that fluctuating estrogen concentrations would affect the crosstalk between L and EC cells, and two periods in the female life cycle come to mind– surges in estrogen during the menstrual cycle, and the meteoric rise in estrogen during late stages of pregnancy (40). Taken together with recent studies that have begun to define molecular cues promoting villus expansion in the maternal gut (41, 42), our findings raise the possibility of yet another essential adaptation to enhance progeny well-being– namely, heightened surveillance of ingested nutrients. Identifying this protective signaling mechanism brings us closer to understanding how hormones and diet, when coupled with stress and inflammatory events, could become maladaptive, leading to chronic visceral pain.

Supplementary Material

Refer to Web version on PubMed Central for supplementary material.

ACKNOWLEDGMENTS

We thank the Garvan Institute, Australia, for genotyping services and the Preclinical, Imaging and Research Laboratories (PIRL, SAHMRI) for the use of their small animal facility; we also thank the UCSF Nikon Imaging Core for use of their confocal imaging facilities, and R. S. Elmes for assistance in FACS analyses. We thank C. Goodman for help with the initial characterization of ERα (*Esr1*^{Vil1Cre}) mutant mice, and J. Bayrer, Z. Torok, K. Touhara, and S. Mohr for many helpful suggestions and critical comments during these studies. We also thank W. Imlach, D. Bohórquez, and L. Jan for sharing the transgenic mice used in this manuscript.

Funding:

This work was supported by the following: NIH Training grant T32 DK007418 and NIGMS K12GM081266-17 (to E.E.F.); NIDDK R01 DK135714 (to H.A.I., D.J., S.M.B.); NINDS R35 NS105038 (to D.J.); NHMRC of Australia Investigator Leadership grant APP2008727 (to S.M.B.); NHMRC Development Grant APP2014250 (to S.M.B.); NHMRC Ideas grant APP2029332 (to J.C.)

Data and materials availability:

RNA-seq datasets have been deposited at GEO (https://www.ncbi.nlm.nih.gov/geo/) under the SuperSeries accession number GEO: GSE306665. This is the author's version of the work. It is posted here by permission of the AAAS for personal use, not for redistribution. The definitive version was published in Science on 18 Dec 2025, DOI: 10.1126/science.adz1398.

REFERENCES AND NOTES

1. Ray J, LaBundy J, Lower Gastrointestinal Tract Disorders: Clinical Updates in Women's Health Care Primary and Preventive Care Review. Obstet Gynecol 139, 1201 (2022). [PubMed: 35675626]
2. Ford AC, Sperber AD, Corsetti M, Camilleri M, Irritable bowel syndrome. Lancet 396, 1675–1688 (2020). [PubMed: 33049223]
3. Houghton LA, Lea R, Jackson N, Whorwell PJ, The menstrual cycle affects rectal sensitivity in patients with irritable bowel syndrome but not healthy volunteers. Gut 50, 471–474 (2002). [PubMed: 11889064]
4. Bernstein MT et al. , Gastrointestinal symptoms before and during menses in healthy women. BMC Womens Health 14, 14 (2014). [PubMed: 24450290]
5. Bayrer JR et al. , Gut enterochromaffin cells drive visceral pain and anxiety. Nature 616, 137–142 (2023). [PubMed: 36949192]
6. Bellono NW et al. , Enterochromaffin Cells Are Gut Chemosensors that Couple to Sensory Neural Pathways. Cell 170, 185–198 e116 (2017). [PubMed: 28648659]
7. Makadia PA et al. , Optogenetic Activation of Colon Epithelium of the Mouse Produces High-Frequency Bursting in Extrinsic Colon Afferents and Engages Visceromotor Responses. J Neurosci 38, 5788–5798 (2018). [PubMed: 29789376]
8. Drucker DJ, GLP-1-based therapies for diabetes, obesity and beyond. Nat Rev Drug Discov 24, 631–650 (2025). [PubMed: 40281304]
9. Lund ML et al. , Enterochromaffin 5-HT cells - A major target for GLP-1 and gut microbial metabolites. Mol Metab 11, 70–83 (2018). [PubMed: 29576437]
10. Batterham RL et al. , Inhibition of food intake in obese subjects by peptide YY3–36. N Engl J Med 349, 941–948 (2003). [PubMed: 12954742]
11. Batterham RL et al. , Gut hormone PYY(3–36) physiologically inhibits food intake. Nature 418, 650–654 (2002). [PubMed: 12167864]
12. Tschop M et al. , Physiology: does gut hormone PYY3–36 decrease food intake in rodents? Nature 430, 1–3 (2004).
13. Wortley KE et al. , Peptide YY regulates bone turnover in rodents. Gastroenterology 133, 1534–1543 (2007). [PubMed: 17920065]
14. Tschop MH, Ravussin E, Peptide YY: obesity's cause and cure? Am J Physiol Endocrinol Metab 293, E1131–1133 (2007). [PubMed: 17848627]
15. Sloth B, Davidsen L, Holst JJ, Flint A, Astrup A, Effect of subcutaneous injections of PYY1–36 and PYY3–36 on appetite, ad libitum energy intake, and plasma free fatty acid concentration in obese males. Am J Physiol Endocrinol Metab 293, E604–609 (2007). [PubMed: 17566112]
16. Halatchev IG, Cone RD, Peripheral administration of PYY(3–36) produces conditioned taste aversion in mice. Cell Metab 1, 159–168 (2005). [PubMed: 16054059]
17. Alonso AM et al. , The vagus nerve mediates the physiological but not pharmacological effects of PYY(3–36) on food intake. Mol Metab 81, 101895 (2024). [PubMed: 38340808]
18. Sainsbury A et al. , Important role of hypothalamic Y2 receptors in body weight regulation revealed in conditional knockout mice. Proc Natl Acad Sci U S A 99, 8938–8943 (2002). [PubMed: 12072562]

19. Keire DA et al. , Primary structures of PYY, [Pro(34)]PYY, and PYY-(3–36) confer different conformations and receptor selectivity. Am J Physiol Gastrointest Liver Physiol 279, G126–131 (2000). [PubMed: 10898754]
20. Kojima S, Tohei A, Ikeda M, Anzai N, An Endogenous Tachykinergic NK2/NK3 Receptor Cascade System Controlling the Release of Serotonin from Colonic Mucosa. Curr Neuropharmacol 13, 830–835 (2015). [PubMed: 26630961]
21. Gustafsson JK, Greenwood-Van Meerveld B, Amygdala activation by corticosterone alters visceral and somatic pain in cycling female rats. Am J Physiol Gastrointest Liver Physiol 300, G1080–1085 (2011). [PubMed: 21454447]
22. Ji Y, Tang B, Traub RJ, The visceromotor response to colorectal distention fluctuates with the estrous cycle in rats. Neuroscience 154, 1562–1567 (2008). [PubMed: 18550290]
23. Bouin M et al. , Rectal distention testing in patients with irritable bowel syndrome: sensitivity, specificity, and predictive values of pain sensory thresholds. Gastroenterology 122, 1771–1777 (2002). [PubMed: 12055583]
24. Ryan JP, Bhojwani A, Colonic transit in rats: effect of ovariectomy, sex steroid hormones, and pregnancy. Am J Physiol 251, G46–50 (1986). [PubMed: 3728676]
25. Handgraaf S, Dusaulcy R, Visentin F, Philippe J, Gosmain Y, 17-beta Estradiol regulates proglucagon-derived peptide secretion in mouse and human alpha- and L cells. JCI Insight 3, DOI: 10.1172/jci.insight.98569 (2018).
26. Hayashi M et al. , Enteroendocrine cell lineages that differentially control feeding and gut motility. Elife 12, DOI: 10.7554/eLife.78512 (2023).
27. Touhara KK et al. , Topological segregation of stress sensors along the gut crypt-villus axis. Nature 640, 732–742 (2025). [PubMed: 39939779]
28. Deng F et al. , Improved green and red GRAB sensors for monitoring spatiotemporal serotonin release in vivo. Nat Methods 21, 692–702 (2024). [PubMed: 38443508]
29. Brenner DM, Sayuk GS, Current US Food and Drug Administration-Approved Pharmacologic Therapies for the Treatment of Irritable Bowel Syndrome with Diarrhea. Adv Ther 37, 83–96 (2020). [PubMed: 31707713]
30. Billesbolle CB et al. , Structural basis of odorant recognition by a human odorant receptor. Nature 615, 742–749 (2023). [PubMed: 36922591]
31. Pluznick JL et al. , Olfactory receptor responding to gut microbiota-derived signals plays a role in renin secretion and blood pressure regulation. Proc Natl Acad Sci U S A 110, 4410–4415 (2013). [PubMed: 23401498]
32. Nishida A, Miyamoto J, Shimizu H, Kimura I, Gut microbial short-chain fatty acids-mediated olfactory receptor 78 stimulation promotes anorexigenic gut hormone peptide YY secretion in mice. Biochem Biophys Res Commun 557, 48–54 (2021). [PubMed: 33862459]
33. Dinsart G et al. , The olfactory receptor Olfr78 promotes differentiation of enterochromaffin cells in the mouse colon. EMBO Rep 25, 304–333 (2024). [PubMed: 38177905]
34. Koo A et al. , Expression of the relaxin family peptide 4 receptor by enterochromaffin cells of the mouse large intestine. Cell Tissue Res 389, 1–9 (2022). [PubMed: 35596811]
35. Taylor BK et al. , Inflammation enhances Y1 receptor signaling, neuropeptide Y-mediated inhibition of hyperalgesia, and substance P release from primary afferent neurons. Neuroscience 256, 178–194 (2014). [PubMed: 24184981]
36. Triadafilopoulos G, Finlayson M, Grellet C, Bowel dysfunction in postmenopausal women. Women Health 27, 55–66 (1998). [PubMed: 9796084]
37. Staudacher HM, Whelan K, The low FODMAP diet: recent advances in understanding its mechanisms and efficacy in IBS. Gut 66, 1517–1527 (2017). [PubMed: 28592442]
38. Hassan AM et al. , Visceral hyperalgesia caused by peptide YY deletion and Y2 receptor antagonism. Sci Rep 7, 40968 (2017). [PubMed: 28106168]
39. Billing LJ et al. , Single cell transcriptomic profiling of large intestinal enteroendocrine cells in mice - Identification of selective stimuli for insulin-like peptide-5 and glucagon-like peptide-1 co-expressing cells. Mol Metab 29, 158–169 (2019). [PubMed: 31668387]
40. Schock H et al. , Hormone concentrations throughout uncomplicated pregnancies: a longitudinal study. BMC Pregnancy Childbirth 16, 146 (2016). [PubMed: 27377060]

41. Onji M et al. , RANK drives structured intestinal epithelial expansion during pregnancy. Nature 637, 156–166 (2025). [PubMed: 39633049]
42. Ameku T et al. , Growth of the maternal intestine during reproduction. Cell 188, 2738–2756 e2722 (2025). [PubMed: 40112802]
43. Babey ME et al. , A maternal brain hormone that builds bone. Nature 632, 357–365 (2024). [PubMed: 38987585]
44. Hockley JR et al. , Visceral and somatic pain modalities reveal Na(V) 1.7-independent visceral nociceptive pathways. J Physiol 595, 2661–2679 (2017). [PubMed: 28105664]
45. Schonhoff S et al. , Energy homeostasis and gastrointestinal endocrine differentiation do not require the anorectic hormone peptide YY. Mol Cell Biol 25, 4189–4199 (2005). [PubMed: 15870288]
46. Brierley SM, Jones RC 3rd, Gebhart GF, Blackshaw LA, Splanchnic and pelvic mechanosensory afferents signal different qualities of colonic stimuli in mice. Gastroenterology 127, 166–178 (2004). [PubMed: 15236183]
47. Matikainen-Ankney BA et al. , An open-source device for measuring food intake and operant behavior in rodent home-cages. Elife 10, DOI: 10.7554/eLife.66173 (2021).
48. Wilson SS et al. , Optimized Culture Conditions for Improved Growth and Functional Differentiation of Mouse and Human Colon Organoids. Front Immunol 11, 547102 (2020). [PubMed: 33643277]
49. Dobin A et al. , STAR: ultrafast universal RNA-seq aligner. Bioinformatics 29, 15–21 (2013). [PubMed: 23104886]
50. Liao Y, Smyth GK, Shi W, featureCounts: an efficient general purpose program for assigning sequence reads to genomic features. Bioinformatics 30, 923–930 (2014). [PubMed: 24227677]
51. Love MI, Huber W, Anders S, Moderated estimation of fold change and dispersion for RNA-seq data with DESeq2. Genome Biol 15, 550 (2014). [PubMed: 25516281]

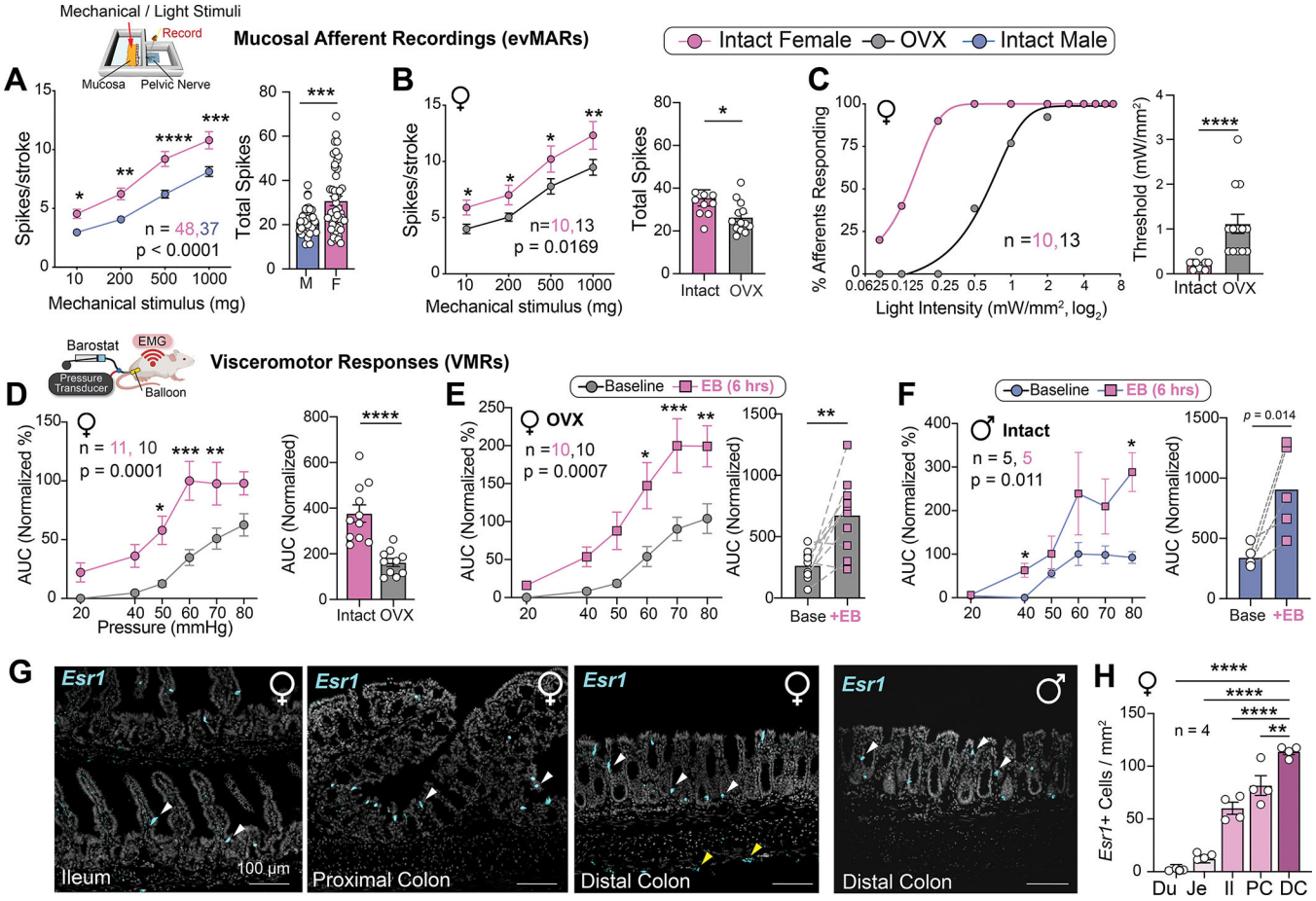

Fig. 1. Estrogen heightens visceral sensitivity in females and is enriched in the distal colon.

(**A**) Mucosal afferent recordings (evMAR) from intact females and males to mucosal stroking (left). $n = 37$ to 48 afferents. Two-way repeated measures analysis of variance (ANOVA) followed by Šidák's multiple comparisons test for each stimulus-response pair, $*P < 0.05$, $**P < 0.01$, $***P < 0.001$, $****P < 0.0001$. Total number of evMAR spikes (right). Unpaired *t*-test, $***P < 0.001$. (**B**) evMAR responses in intact and OVX females (left). $n = 10$ to 13 afferents. Two-way repeated measures ANOVA followed by Bonferroni multiple comparisons test, $*P < 0.05$, $**P < 0.01$. Total number of evMAR spikes (right). Unpaired *t*-test, $*P < 0.05$. (**C**) Percentage of mucosal afferents responding at indicated light intensities (left), and activation thresholds of afferents (right) in intact and OVX *$Na_V1.8$-ChR2* female mice. $n = 10$ to 13 afferents. Nonlinear regression and the Mann-Whitney test were used, respectively, with $****P < 0.0001$. (**D**) VMR responses (left) and total area under the curve (AUC) (right) for intact and OVX females. $n = 11$, 10 mice. Two-way repeated measures ANOVA followed by Šidák's multiple comparisons test (left) and paired *t*-test (right). $*P < 0.05$, $**P < 0.01$, $***P < 0.001$, $****P < 0.0001$. (**E**) Using the same OVX female cohort from (D), VMR responses at 6 hours following EB injections (1 µg per mouse) are shown. $n = 10$ mice. Two-way repeated measures ANOVA followed by Šidák's multiple comparisons test (left), paired *t*-test (right). $*P < 0.05$, $**P < 0.01$. (**F**) VMR responses (left) and total AUC (right) for intact males at baseline and 6 hours following EB treatment (1 µg per mouse). Two-way repeated measures ANOVA followed by Šidák's multiple comparisons

test (left), paired *t*-test (right), $*P < 0.05$. (**G**) *Esr1* transcripts visualized in the ileum, proximal, and distal colon, epithelial expression (white arrowheads) and neuronal expression (yellow arrowheads). Scale bars, 100 μm. (**H**) Plot of *Esr1*+ cell density quantified from 15 fields per intestinal segment (Du, duodenum; Je, jejunum; Il, ileum; PC, proximal colon; DC, distal colon). $n = 4$ mice. Nested one-way ANOVA followed by Dunnett's multiple comparisons test, $**P < 0.01$, $****P < 0.0001$. VMRs were normalized to maximal responses in intact females (D), OVX females (E), and males (F). The evMAR and VMR schematics were created by the authors, and part of the VMR schematic was rendered using BioRender.com. Data are presented as mean ± SEM.

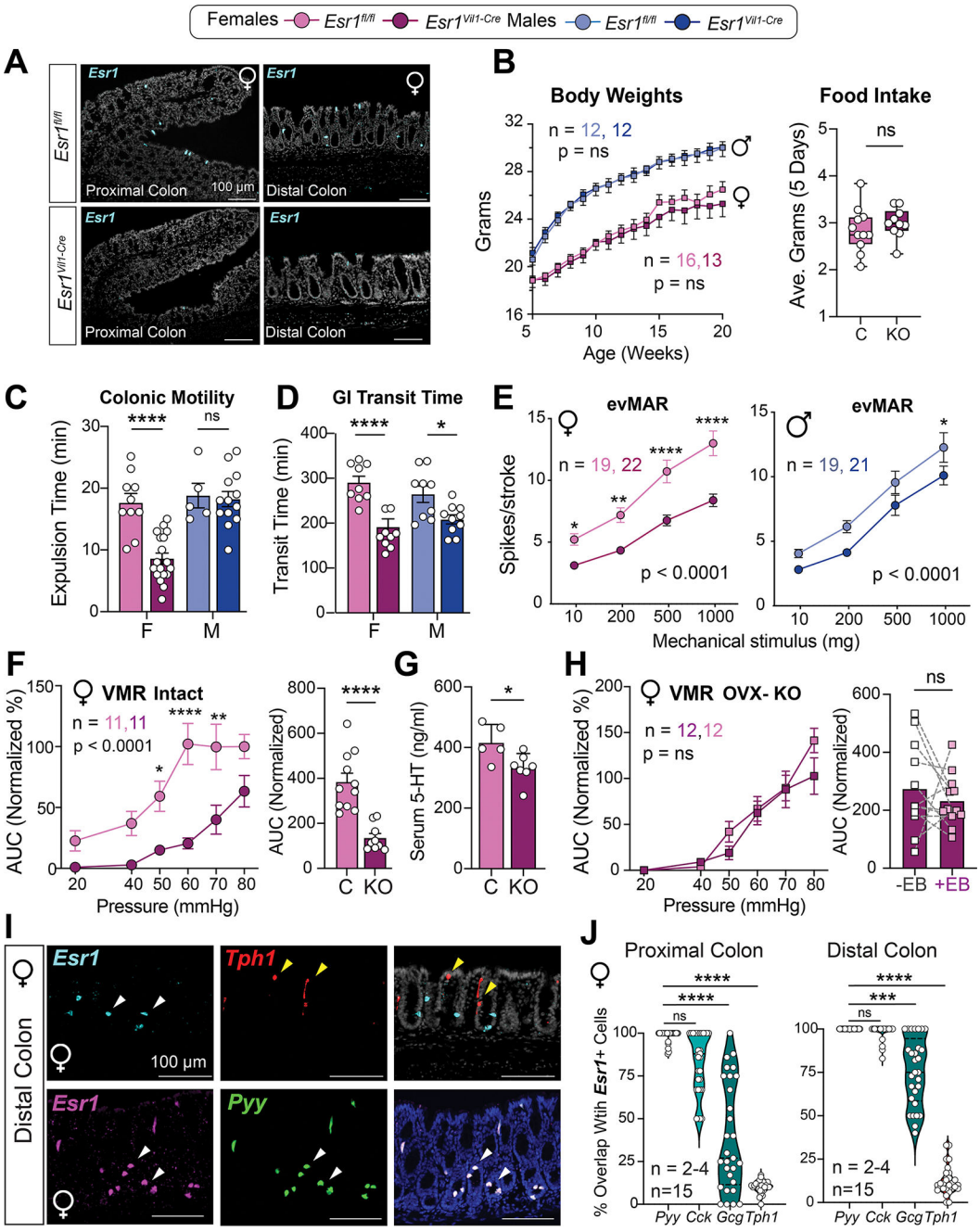

Fig. 2. ERα signaling is restricted to PYY^{+} L cells and is required for normal gut motility and female visceral sensitivity.

(**A**) *Esr1* expression in the proximal and distal colons of *Esr1*$^{fl/fl}$ and *Esr1*$^{Vil1\text{-}Cre}$ female mice. Scale bars, 100 µm. (**B**) Post-weaning body weights from 5 to 20 weeks in *Esr1*$^{fl/fl}$ and *Esr1*$^{Vil1\text{-}Cre}$ females and males (left); average food intake over a 5-day period in *Esr1*$^{fl/fl}$ and *Esr1*$^{Vil1\text{-}Cre}$ females (right). n = 12 to 16 mice. Two-way repeated measures ANOVA (left) and unpaired two-tailed *t*-test (right); n.s., not significant. (**C**) Colonic bead expulsion time in *Esr1*$^{fl/fl}$ and *Esr1*$^{Vil1\text{-}Cre}$ females (F) and males (M). n = 5 to 18 mice. Unpaired 2-tailed t-tests. **** $P < 0.0001$; n.s., not significant. (**D**) GI transit times in *Esr1*$^{fl/fl}$ and *Esr1*$^{Vil1\text{-}Cre}$

females (F) and males (M). $n = 9$ to 10 mice. Unpaired 2-tailed t-tests. $*P < 0.05$, $****P < 0.0001$. (**E**) evMAR responses in $Esr1^{Vil1\text{-}Cre}$ and $Esr1^{fl/fl}$ females and males. $n = 19$ to 22 afferents. Two-way repeated measures ANOVA followed by Šidák's multiple-comparisons test. $*P < 0.05$, $**P < 0.01$, $****P < 0.0001$. (**F**) VMR responses and total AUC in intact $Esr1^{fl/fl}$ controls and $Esr1^{Vil1\text{-}Cre}$ females. $n = 9$ to 11 mice. Two-way repeated measures ANOVA followed by Šidák's multiple-comparisons test (left) and unpaired two-tailed *t*-test (right). $*P < 0.05$, $**P < 0.01$, $****P < 0.0001$. (**G**) Circulating 5-hydroxytryptamine (5-HT) concentrations in $Esr1^{fl/fl}$ and $Esr1^{Vil1\text{-}Cre}$ females, unpaired two-tailed *t*-test, $*P < 0.05$, $n = 5$ to 7 mice. (**H**) VMR data in OVX $Esr1^{Vil1\text{-}Cre}$ females at baseline and following EB injections (1 μg per mouse). $n = 9$ to 10 mice. Two-way repeated measures ANOVA followed by Šidák's multiple-comparisons test (left) and Wilcoxon matched-pairs signed-rank two-tailed test (right); n.s., not significant. **(I)** Images of distal colons from female mice showing *Esr1*-positive cells (white arrowheads) showing expression of *Pyy* (bottom panel), but not *Tph1* transcripts (top panel; yellow arrowheads). Scale bars, 100 μm. (**J**) Quantification of colonic *Esr1+* cells co-expressing *Pyy* ($n = 4$ mice), *Cck*, *Gcg*, and *Tph1* ($n = 2$ mice) across 15 fields per colonic segment. Nested one-way ANOVA followed by Dunnett's multiple comparisons test. $**P < 0.01$, $****P < 0.0001$. VMRs were normalized to maximal responses in intact females (F) and KO females (H). Data are presented as mean ± SEM.

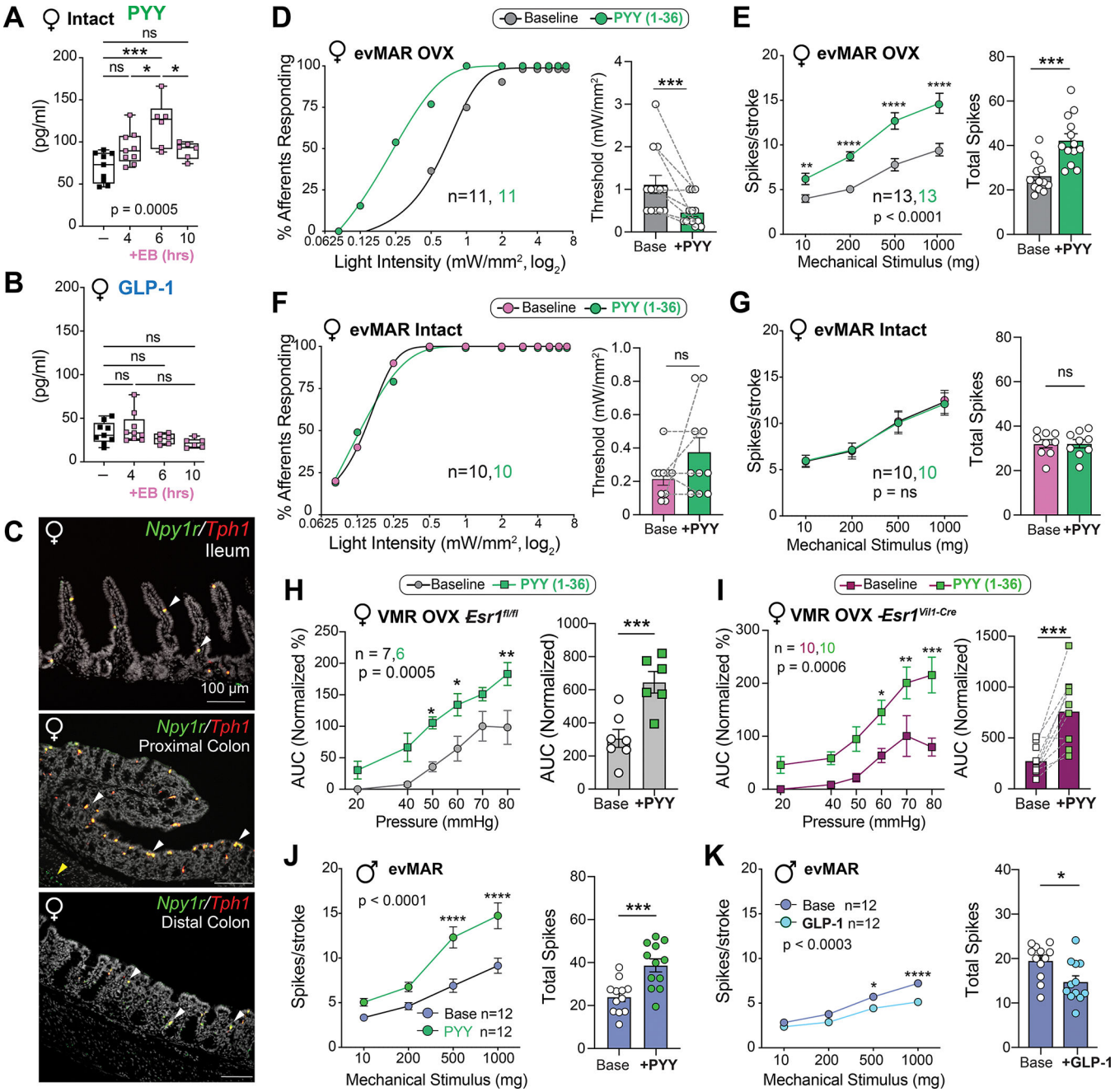

Fig. 3. $PYY_{1–36}$ but not GLP-1, acts downstream of ERa signaling to promote visceral sensitivity.

(**A**) Circulating PYY concentrations and **(B)** circulating GLP-1 concentrations in female mice at baseline and following 4, 6, and 10 hours of EB (1 µg per mouse) treatment. $n = 6$ to 9 mice. One-way ANOVA followed by Tukey's multiple comparisons test. $*P < 0.05$, $***P < 0.001$; n.s., not significant. (**C**) Representative images of *Npy1r* expression in *Tph1*+ EC cells visualized in the ileum, proximal, and distal colon (co-expression indicated by white arrows and neuronal expression by the yellow arrow). Scale bars, 100 µm. (**D**) Percentage of mucosal afferents responding at indicated light intensities (left), and activation thresholds of afferents (right) in OVX *$Na_V1.8$-ChR2* females at baseline and following $PYY_{1–36}$ treatment

(30 nM), $n = 11$ afferents. Nonlinear regression (left) and Wilcoxon matched-pairs signed-rank two-tailed test (right). ***$P < 0.001$. (**E**) evMAR responses in OVX *$Na_V1.8$-ChR2* females at baseline and following $PYY_{1–36}$ treatment (30 nM), $n = 13$ afferents. Two-way repeated measures ANOVA followed by Bonferroni multiple comparisons test (left) and unpaired two-tailed *t*-test (right). **$P < 0.01$, ***$P < 0.001$, ****$P < 0.0001$. (**F**) Same as (D) but in intact *$Na_V1.8$-ChR2* females at baseline following $PYY_{1–36}$ treatment. $n = 10$ afferents. Nonlinear regression (left) and Wilcoxon matched-pairs signed-rank two-tailed test (right); n.s., not significant. (**G**) Same as (E) but in intact *$Na_V1.8$-ChR2* females at baseline and following $PYY_{1–36}$ treatment. $n = 10$ afferents. Two-way repeated measures ANOVA followed by Bonferroni multiple comparisons test (left) and unpaired two-tailed *t*-test (right); n.s., not significant. (**H** and **I**) VMR responses and total AUC at baseline and after $PYY_{1–36}$ treatment (10 μg/kg) in OVX *$Esr1^{fl/fl}$* control (H) and *$Esr1^{Vil1\text{-}Cre}$* KO (I) females. $n = 6$ to 10 mice. Two-way repeated measures ANOVA followed by Šidák's multiple-comparisons test (left) and unpaired two-tailed *t*-test in (H) (right) and paired two-tailed *t*-test in (I) (right) *$P < 0.05$, **$P < 0.01$, ***$P < 0.001$, ****$P < 0.0001$. (**J** and **K**) evMAR responses in males at baseline and following $PYY_{1–36}$ (J) or $GLP\text{-}1_{7–36}$ (100 nM) (K) treatment. $n = 12$ afferents. Two-way repeated measures ANOVA followed by Bonferroni multiple comparisons test (left) and unpaired two-tailed *t*-test (right). *$P < 0.05$, ***$P < 0.001$, ****$P < 0.0001$. Data are presented as mean ± SEM. VMRs were normalized to maximal responses to OVX females (H) and KO females (I).

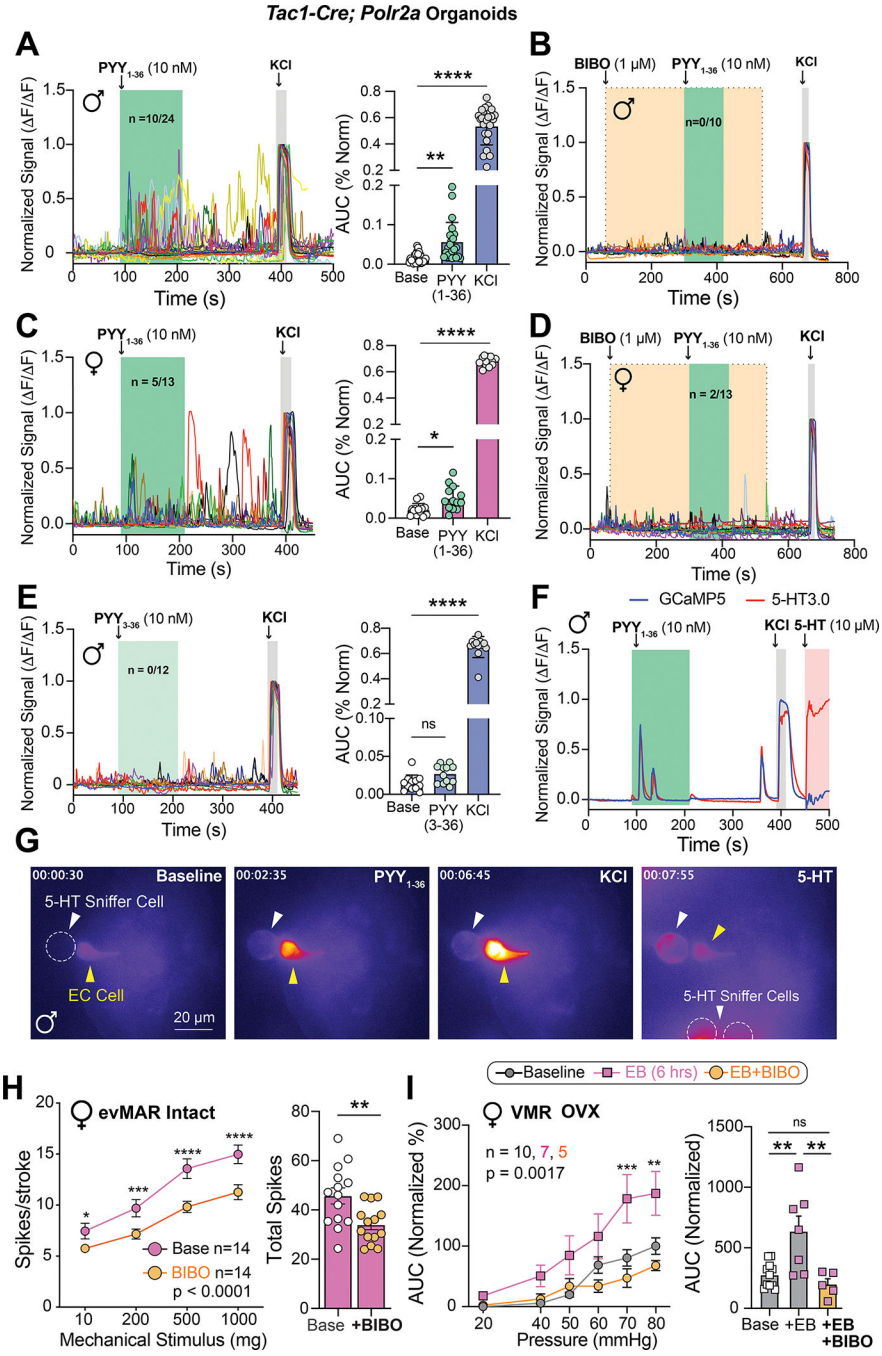

Fig. 4. $PYY_{1–36}$ promotes 5-HT release from EC cells and enhances visceral sensitivity via NPY1R.

(A) $PYY_{1–36}$ (10 nM)-evoked calcium responses in EC cells within male intestinal organoids from *Tac1*^{Cre};*Polr2a*$^{(GCaMP5g\text{-}IRES\text{-}tdTomato)}$ mice. Responses are shown for each individual EC cell normalized to the maximal activation with KCl, with the number of responders indicated in the figure panel, $n = 24$ cells. Kruskal-Wallis test followed by Dunn's multiple comparisons test, $^{**}P < 0.01$, $^{****}P < 0.0001$. (**B**) Effects on calcium responses in male organoids following BIBO 3304 (1 μM), an NPY1R antagonist,

administered prior to $PYY_{1–36}$, $n = 10$ cells. **(C)** Effects of $PYY_{1–36}$ on female organoids as described in (A). $n = 13$ cells. One-way ANOVA followed by Tukey's multiple comparisons test, $^{*}P < 0.05$, $^{****}P < 0.0001$. (**D**) Effects of BIBO 3304 on female EC cells, $n = 13$ cells. (**E**) $PYY_{3–36}$ effects on calcium responses in male organoids, $n = 12$ cells. One-way ANOVA followed by Dunnett's multiple comparisons test for AUC data. $^{****}P < 0.0001$; n.s., not significant. (**F**) Representative recordings of $gGRAB_{5\text{-}HT3.0}$-expressing HEK293T cells (red) and GCaMP5g-expressing EC cells in male organoids (blue) measuring 5-HT release and Ca^{2+} signals from EC cells in the sniffer experiment. (**G**) Representative frames from live imaging of the $gGRAB_{5\text{-}HT3.0}$ sniffer experiment with 5-HT sniffer cell (white arrowheads) next to a GCaMP5g+ EC cell (yellow arrowheads) in an intestinal organoid. A dashed circle outlines the sniffer cell in the far-left panel. Scale bar, 20 μm. (**H**) evMAR responses (left) and total spikes (right) in intact females at baseline and following BIBO 3304 treatment (1 μM). $n = 14$ afferents. Two-way repeated measures ANOVA followed by Bonferroni multiple comparisons test (left) and two-tailed, unpaired *t*-test (right). $^{*}P < 0.05$, $^{**}P < 0.01$, $^{***}P < 0.001$, $^{****}P < 0.0001$. (**I**) VMR responses and total AUC in the same OVX controls at baseline replotted from Fig. 1E, $n = 11$ mice, or treated with EB (1 μg) or EB + BIBO 3304 (1 mg/kg). $n = 5$ to 7 mice. Two-way repeated measures ANOVA followed by Šidák's multiple comparisons test (left), and one-way ANOVA followed by Tukey's multiple comparisons test (right). $^{*}P < 0.05$, $^{**}P < 0.01$, $^{***}P < 0.001$. Data are presented as mean ± SEM. VMRs were normalized to maximal responses in OVX females (I).

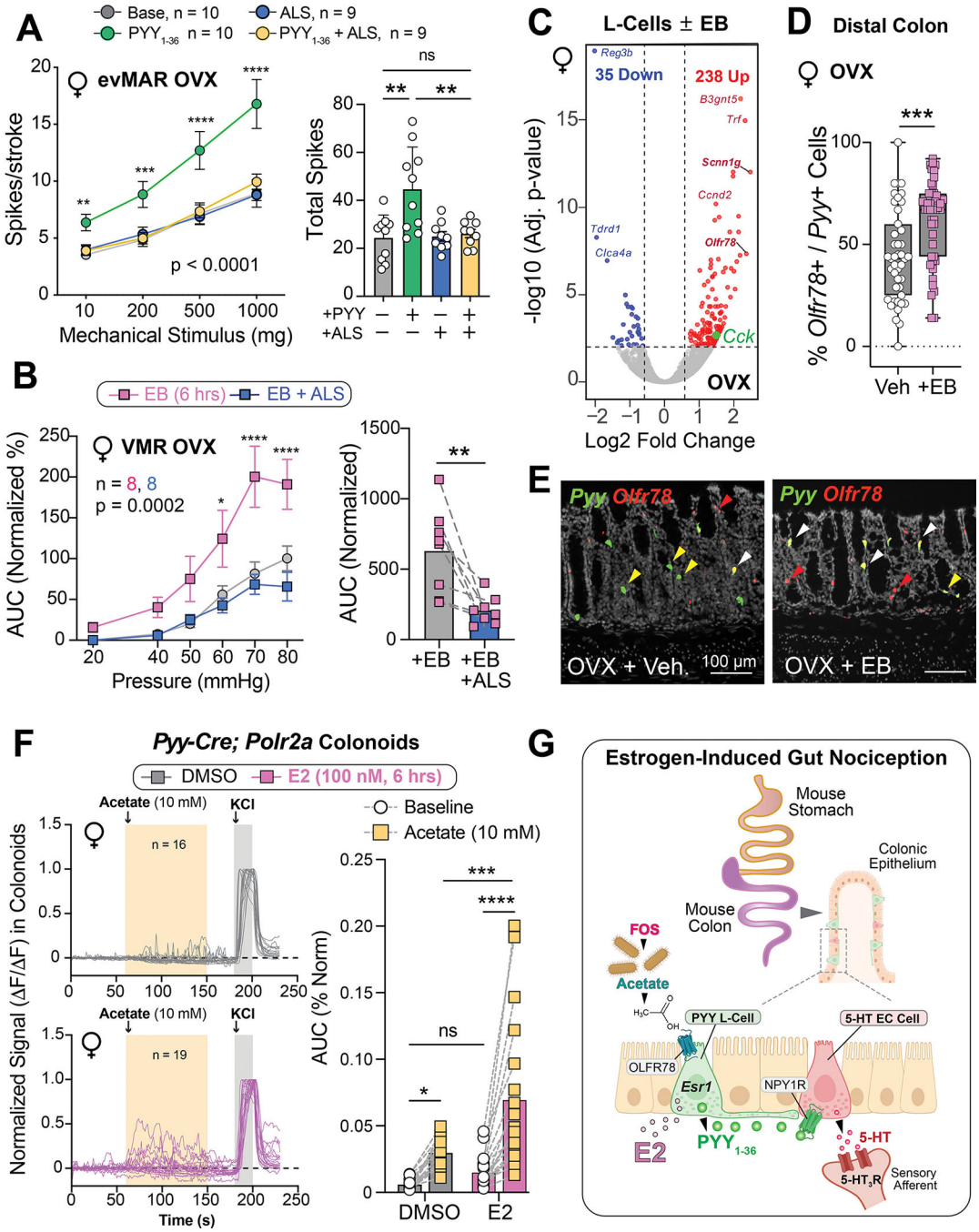

Fig. 5. Estrogen increases SCFA detection in L-cells and engages a potent gut pain pathway.

(**A**) evMAR responses (left) and total spikes (right) in OVX females under four conditions: baseline, $PYY_{1–36}$ (30 nM) treatment only, alosetron (ALS) treatment only (10 µM), and $PYY_{1–36}$ + ALS. $n = 9$ to 10 afferents. Two-way repeated measures ANOVA followed by Bonferroni multiple comparisons test (left) and one-way ANOVA followed by Tukey's multiple comparisons test (right). $^{**}P < 0.01$, $^{***}P < 0.001$, $^{****}P < 0.0001$; n.s., not significant. (**B**) VMR responses and total AUC in OVX controls at baseline or treated with EB (1 µg per mouse) or EB + ALS (0.1 mg/kg). $n = 5$ to 7 mice. Two-way repeated

measures ANOVA followed by Šidák's multiple comparisons test (left), and one-tailed, paired *t*-test (right). **P* < 0.05, ***P* < 0.01, *****P* < 0.0001. (**C**) Volcano plot showing changes in mRNA expression profile of L cells in response to 4 hours of EB treatment, upregulated genes (red), downregulated genes (blue). (**D**) Quantification of percent of cells coexpressing *Pyy* and *Olfr78* in distal colons of OVX mice treated with vehicle (Veh) or estradiol benzoate [(EB), 1 μg per mouse]. *n* = 3 mice per group. Nested unpaired two-tailed *t*-test. ****P* < 0.001. (**E**) Representative images of distal colons showing *Olfr78* receptor expression in L cells from OVX mice treated with vehicle or EB. Cells expressing primarily *Pyy* (yellow arrowheads), solely *Olfr78* (red arrowheads), and overlapping Pyy/Olfr78 (white arrowheads). Scale bars, 100 μm. (**F**) Normalized fluorescent responses from L cells expressing GCaMP5g at baseline (10 mM NaCl), and after application of acetate (10 mM), and high KCl in colonoids derived from Pyy^{Cre};$Polr2a^{(GCaMP5g\text{-}IRES\text{-}tdTomato)}$ female mice preincubated with vehicle or estradiol (E2, 100 nM) for 6 hours. *n* = 16 to 19 cells. Bar graphs for matched pairs of cells before and after treatment. Two-way ANOVA, mixed effects analyses. **P* < 0.05, ****P* < 0.001, *****P* < 0.0001; n.s., not significant. (**G**) Estrogen initiates paracrine signaling between L and EC cells in the female colonic epithelium, affecting visceral sensitivity. Estradiol acting through ERa in L-cells upregulates *Olfr78* expression, increasing its response to bacterial acetate produced from fermentable oligosaccharides (FOS) and leading to $PYY_{1–36}$ release (32). $PYY_{1–36}$ then acts on NPY1R in EC cells, resulting in activation of 5-HT_3R-expressing sensory nerve fibers to transduce pain information to the central nervous system. Data are presented as mean ± SEM. VMRs were normalized to maximal responses to OVX females (B). The model in (G) was partially rendered using BioRender.com.